ISSN: 1687-1006 p
ISSN: 2682-3640 e

The Egyptian International Journal of Engineering Sciences and Technology

https://eijest.journals.ekb.eg/

Vol. 41 (2023) 27–39

DOI: 10.21608/eijest.2022.136365.1154

Kaolin-Metakaolin Crystallographic Transformation and the Durability of Metakaolin-Based Geopolymer Concrete

Yetunde O. Abiodun[a*], Samson O. Adeosun[b,c]

[a]*Department of Civil and Environmental Engineering, University of Lagos, Nigeria.*
[b]*Department of Metallurgical and Materials Engineering, University of Lagos, Nigeria.*
[c]*Industrial Engineering Department, Durban University of Technology, Durban, South Africa.*

ARTICLE INFO

Article history:

Received 28 April 2022
Received in revised form
19 June 2022
Accepted 9 July 2022
Available online 9 July 2022

Keywords:

Calcination
Crystallography
Durability
Geopolymer
Metakaolin

ABSTRACT

The quest to reduce and eliminate the resultant health hazards posed by the continued use of cement in structural works has led to the emergence of metakaolin-based geopolymer as a viable alternative to cement. Kaolin was explored as a material for metakaolin production from four Nigerian deposits: Imeko, Okpela, Ifon and Isan-Ekiti. Metakaolin was obtained by calcining kaolin samples at temperatures ranging from 500°C to 1000°C for 30, 60, 120, and 180 minutes at an interval of 100°C. ImageJ software was used to measure the area of particles present in each sample micrograph obtained from Scanning electron microscopy. The metakaolin samples were also subjected to atomic absorption spectroscopy and X-ray diffraction examinations. Metakaolin samples were classed as class N pozzolan and X-ray diffraction spectroscopy revealed the presence of amorphous silica in metakaolin and distinct crystal systems were detected using a crystallography test on the samples. The chloride permeability test according to ASTM C1202 indicated that Metakaolin-based geopolymer concrete (Mk-GPC) showed a significant decrease in the charges passing through at 28 days when compared to 90 days. This trend was similar to the result obtained from OPC-concrete when charges were passed through the samples. This shows that both Mk-GPC and OPC-concrete can be considered acceptable for the protection of embedded steel reinforcement from corrosion in real-life construction works as they have good resistance to chloride permeability. According to this research finding, metakaolin-based geopolymer could be used as a sustainable alternative to cement in Nigeria.

1. Introduction

According to the World Business Council for Sustainable Development study [1], global cement production is expected to reach 4.4 billion metric tons by 2050, implying that the cement industry would contribute around 5-7 percent of world CO_2 emissions [2]. In the light of this, researchers and industries are now considering the use of alternative materials to cement by partially replacing it with pozzolans such as fly ash, rice husk ash, or completely replacing cement with novel binders such as metakaolin (a geopolymer). Geopolymer binders are associated with little or no carbon dioxide emission in their production and are therefore termed green cement or green technology [3]. Kaolin clay

* Corresponding author. Tel.: +2348034403886
E-mail address: yabiodun@unilag.edu.ng

from which metakaolin is obtained through the calcination process can be found in large quantities in soils created by the chemical weathering of rocks in tropical rainforest areas with a hot and humid climate. Kaolin is present in varying amounts in other minerals such as muscovite, quartz, feldspar, and anatase. Though, there are many forms of kaolin and many ways to process it, one of the most common is calcining kaolin to obtain metakaolin at a controlled and appropriate temperature. It is critical to understand that the mineralogical spectrum of the crude kaolin and the required end products dictate the type of process to be used [4]. Metakaolin was used as a substitute for cement in this investigation. Metakaolin is a prime product, not a by-product as the processes from kaolin to metakaolin are well-structured to produce a reactive material. Metakaolin is typically created by calcining kaolin clay at temperatures ranging from 600°C to 800°C to refine its color, remove inert impurities, and tune particle size [5]. Geopolymers are inorganic binders created by combining natural pozzolanic materials and amorphous aluminosilicates, such as coal ash and metakaolin, with alkali activators, such as water glass, NaOH, or KOH [6, 7]. The structure of a geopolymer is built up of randomly linked Si tetrahedrons with part of their Si cations replaced with Al, and the charge imbalance induced by the cation substitutions is balanced out by alkali earth metals found in alkali activators [8]. Geopolymers are noted for having exceptional mechanical properties such preliminary compressive strength, thermal resistance, and water permeability, as well as good chemical properties like acid resistance and hazardous element resistance, when compared to Portland cement [9, 10]. Furthermore, unlike cement, it does not require a high-temperature sintering process, resulting in lower carbon dioxide emissions [6]. Metakaolin improves the strength and durability of concrete [11], has a filler effect, accelerates the hydration of Ordinary Portland Cement (OPC), and has pozzolanic properties when treated with calcium hydroxide [12]. OPC-concrete structures are universally used in construction works and perform satisfactorily for most civil engineering structures. However, the production of cement, which is a crucial constituent in OPC-concrete requires a high temperature and causes the emission of greenhouse gas that is harmful to the environment leading to health problems and climate change [13]. Therefore, there is a serious need for developing alternative and eco-friendly materials to avoid these shortcomings of cement. Incidentally, geopolymer concretes are potential materials [14] that have been developed. Some of these new concretes are made from industrial wastes like fly ash and pulverized granulated blast furnace slag, while others are made from natural mineral resources like kaolin [15].

Table 1. Kaolin deposits and their estimated reserves in Nigeria

Mineral	States	Site Locations	Estimated Reserve (Million tonnes)
Kaolin	Edo	Okpela, Igbanke, Ozonnogogo	Very large
	Plateau	Jos, Barkin-Ladi, Kanke, Bassa	19
	Niger	Pategi, Kpaki, Mokwa, Paikoroi	Very large
	Katsina	Kankara, Ingawa, Batsari, Batagarawa,Dutsin-Ma	20
	Ogun	Oshide, Imeko, Ipokia	Large
	Bauchi	Darazo	18
	Oyo	Iseyin, Saki – West and East, Atisbo	2
	Sokoto	Illo	2.5
	Ondo	Ifon, Irele, Odigba	N.A
	Anambra	Ozubulu, Aguata, Ayamelum, Ihiala	4.2
	Ekiti	Isan- Ekiti, Ikere-Ekiti	3
	Kaduna	Maraban-Rido	5.5
	Benue	Obi, Ogbadibo, Oturkpo	10
	Borno	Damboa, Chibok, Gwoza	Large
	Enugu	Enugu	50
	Kebbi	Bagudo, Suru, Wasagu/Danko	Very large
	Abia	Nneochi, Obingwa, Isikwuato, Ikwuano	Very large
	Kwara	Baruten, Edu, Isin, Kaiama, Ifelodun	Large

Nigeria has an estimated reserve of about two (2) billion metric tonnes of kaolin deposits scattered in different parts of the country [16]. Table 1 shows the location of kaolin formations in Nigeria, along with their estimated reserves [17].

2. Materials and Methods

2.1 Materials

Kaolin samples from Ogun (Imeko), Edo (Okpela), Ondo (Ifon), and Ekiti (Isan-Ekiti) states in Nigeria were calcined at temperatures ranging from 500 to

1000°C (at 100°C intervals) and heating durations of 30, 60, 120, and 180 minutes. As described by [18], preliminary examinations were conducted on kaolin samples. The percentage of chemical compounds present in the metakaolin samples at every calcination temperature and duration were obtained through Atomic Absorption spectroscopy (AAS). This investigation was carried out at Sheda Science and Technology Institute, Abuja, Nigeria (SHEDA, Abuja) using the Shimadzu AA-7000 spectrometer model.

2.2 Durability studies

Whiting [19] devised the Rapid Chloride Penetration Test (RCPT), which was later approved as ASTM C1202 [20]. A 60V DC voltage was applied to water-saturated concrete samples with a diameter of 100mm and a thickness of 50mm for 6 hours. As illustrated in Fig. 1, two reservoirs containing 3.0 percent NaCl solution and 0.3M NaOH solution were used for the setup. The resistance of the specimen to chloride-ion penetration was found to be related to the total charge passed in coulombs. The details of this test can be found in ASTM C1202 [20], and the results can be used to evaluate the concrete's durability using the criteria listed in Table 2. The electrical voltage maintained across the specimens forces the chloride ions to penetrate the specimens. The electrical conductivity of concrete is determined in this test to offer a quick estimate of its resistance to chloride ion penetration. As more current travels through a more permeable concrete, its chloride-ion resistance provides an indirect measure of its permeability and interior structure [21]. In this study, the corrosion inclinations of Mk-GPC and OPC-concrete in a chloride environment were compared. Alumino-silicates in Mk-GPC and calcium silicate hydrate in OPC-concrete serve as binders in these two systems. The ASTM 1202 [20] technique was used to determine the structures' chloride permeability.

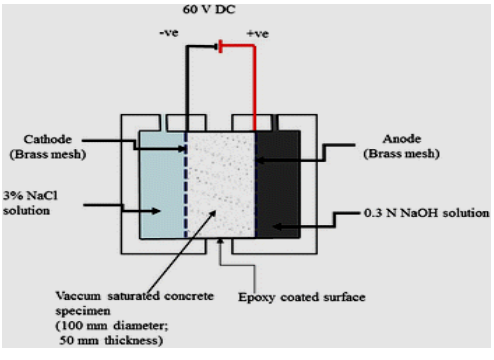

Fig 1. Schematic diagram of RCPT apparatus

Table 2: ASTM C1202 ratings for RCPTs.

Charged passed (Coulombs)	Permeability of Chloride Ions
Above 4000	High
From 2000-4000	Moderate
From 1000-2000	Low
From 100-1000	Very low
Below100	Negligible

In this study, the corrosion inclinations of Mk-GPC and OPC-concrete in a chloride environment were compared. Alumino-silicates in Mk-GPC and calcium silicate hydrate in OPC-concrete serve as binders in these two systems. The ASTM 1202 [20] technique was used to determine the structures' chloride permeability.

2.2.1 Preparation of Specimens

100mm (diameter) x 50mm (thickness) cylindrical specimens were cast for the RCPT. This was employed to determine the resistance to chloride penetration following ASTM C1202 [20]. The selection of ASTM C1202 [20] was done to reduce the test period. The mix proportion in Table 3 was achieved by trial mixes and it ensured that the slump of at least 100mm was obtained. The Mk-GPC samples were cured at ambient conditions while the control samples (OPC-concrete) were cured using the conventional water curing. Six specimens were cast in all and treated at 28-days using the RCPT.

Table 3. Mix proportions of Mk-GPC and OPC- concrete (Control) for RCPT

Mix ID	**Mk-GPC**	**Control**
Binder/Activation solution	0.5	0.5
Binding Agent	Aluminosilicates	Calcium silicate hydrate (C-S-H)gel
Activation solution	Alkaline activators (NaOH & Na_2SiO_3)	
Slump (mm)	125	115
Ingredients (Kg/m^3)		
Metakaolin	162	-
Cement	-	135
Fine Aggregate (Sharp sand)	178	149
Coarse Aggregate (Granite)	421	351

2.3 Crystallographic Transformation of Kaolin to Metakaolin

2.3.1 Scanning Electron Microscopy of metakaolin and X-ray Diffraction of kaolin and metakaolin samples.

The ASPEX 3020 Scanning Electron Microscopy (SEM) was used to investigate the morphology of the selected metakaolin samples, and the images were analyzed using ImageJ. Metakaolin samples were milled for 3 hours after being heated to 800^{O}C for 60 minutes. At the National Geosciences Research Laboratories (NGRL) Kaduna, Nigeria, X-ray diffraction (XRD) of the samples was performed using Empyrean XRD to ensure that the metakaolin samples were unadulterated. A single crystal monochromatic detector and a PIXcel 3D detector are included in the XRD setup. A cathode-ray tube produced the X-rays, which were then filtered to produce monochromatic radiation, collimated to concentrate the beam, and aimed towards the sample. The phases of kaolin and metakaolin samples were determined using XRD (Cu K radiation at 45 kV with a current of 40 mA).

Table 4. Effect of calcining temperature and duration on the chemical composition of Metakaolin samples

Sample		Ogun			Edo			Ekiti			Ondo		
		Chemical compounds											
Tempt (°C)	Time (mins)	SiO_2	Al_2O_3	Fe_2O_3	SiO_2	Al_2O_3	Fe_2O_3	SiO_2	Al_2O_3	Fe_2O_3	SiO_2	Al_2O_3	Fe_2O_3
500	30	48.54	32.80	4.29	47.89	31.69	2.10	42.61	29.09	2.41	40.12	30.98	1.53
	60	48.62	31.45	4.08	48.03	32.74	2.64	44.53	30.10	2.44	41.28	30.43	1.82
	120	48.76	32.88	3.83	48.32	31.74	1.95	46.37	28.39	2.38	42.23	32.24	1.78
	180	48.80	33.45	4.01	48.20	32.54	2.04	45.38	29.73	1.93	44.26	31.08	2.23
600	30	47.34	32.97	3.48	47.91	33.18	1.73	44.43	30.17	2.92	43.28	32.12	1.93
	60	48.47	33.67	2.97	47.63	33.75	1.64	47.28	31.28	3.03	45.23	34.83	1.20
	120	49.50	34.24	2.65	46.54	32.47	2.11	47.52	32.39	2.39	43.29	33.29	1.01
	180	49.54	35.32	3.09	46.18	35.52	1.27	46.93	33.28	3.03	45.11	32.19	0.38
700	30	49.58	34.98	2.74	48.94	33.33	2.27	49.03	29.35	2.36	47.32	34.37	1.38
	60	50.46	35.56	2.27	49.52	35.47	1.36	47.83	28.93	1.63	46.28	35.83	0.87
	120	50.86	35.71	3.04	49.32	36.84	1.21	49.39	29.03	2.45	47.92	34.29	0.74
	180	51.48	36.87	2.31	49.21	36.41	0.92	50.04	27.94	1.28	45.20	35.32	1.83
800	30	52.65	37.82	1.76	50.28	35.94	1.10	53.28	28.43	2.02	47.93	37.29	0.64
	60	**53.49**	**39.90**	**0.52**	**51.60**	**38.30**	**0.54**	**56.21**	**28.89**	**1.29**	**49.92**	**38.98**	**0.39**
	120	53.48	37.23	2.09	49.47	37.29	1.24	56.01	27.93	1.24	48.38	37.77	0.63
	180	53.45	37.10	2.07	50.08	37.10	1.48	55.92	26.38	1.82	48.20	37.38	0.49
900	30	51.06	35.42	3.13	51.12	36.38	1.36	49.37	26.39	2.07	46.29	38.21	0.39
	60	52.78	36.82	3.25	51.21	37.21	0.93	48.83	23.48	2.16	47.18	26.36	0.83
	120	51.32	35.02	2.29	49.28	35.43	0.95	47.69	25.22	1.83	45.32	32.00	1.21
	180	50.41	34.23	3.67	47.66	35.48	1.08	45.33	23.87	1.63	44.46	31.27	1.28
1000	30	50.67	33.42	2.74	45.56	34.08	1.27	47.41	27.39	2.00	45.39	37.28	0.37
	60	51.25	34.26	2.68	46.43	33.03	0.99	45.59	26.05	1.62	46.24	32.10	0,65
	120	50.45	32.21	3.03	43.27	32.87	0.72	43.34	25.33	1.46	44.63	29.03	0.93
	180	49.75	33.46	3.73	44.16	33.90	0.86	46.28	22.01	1.72	39.20	26.22	1.20

3. Results and Discussion

3.1 Effect of varying temperature and time on the chemical composition of metakaolin samples

After subjecting the kaolin samples to temperatures from 500°C to 1000°C, the percentages of the chemical compounds present were determined and the results are shown in Table 4. It was observed that at 800°C/ 60mins calcination, a reduction in loss on ignition (LOI) occurred for all samples. The cumulative percentages of silica, alumina and ferric content at the optimum condition of 800°C/60mins for all samples are >70% and therefore, classified as class N pozzolan [22]. The result obtained from this study was compared to the chemical requirements as stipulated by [22] and presented in Table 5. A comparison of this study's results with other researchers' outcomes is presented in Table 6.

Table 5. Chemical Requirements based on ASTM C618-12a [22]

	Ogun	**Edo**	**Ekiti**	**Ondo**	**ASTM C618-12a [22] specification**	
Chemical Oxides	%	%	%	%	Class N	
SiO_2	53.49	51.60	56.21	49.92	SiO_2 (Silicon dioxide) + Al_2O_3 (Aluminum oxide) + Fe_2O_3 (Iron Oxide)	70.0
Al_2O_3	39.90	38.30	28.89	38.98		
Fe_2O_3	0.52	0.54	1.29	0.39	SO_3	5.0
CaO	0.12	0.22	1.32	1.47	Loss on ignition, %	10.0
MgO	0.21	0.16	2.62	0.18	Max moisture content, %	3.0
Na_2O	0.11	0.21	0.05	0.08		
K_2O	0.53	0.34	0.98	0.93		
SO_3	0.01	0.06	5.02	2.01		
LOI	4.51	2.65	3.57	3.75		
S. gravity	2.40	2.36	2.42	2.48		

Table 6. Comparison with results from other studies

Chemical Oxides (%)	Study Metakaolin at 800ºC/ 60 mins				Gambo *et al*. [24]	Albidah [25]	Ayeni [26]	Edouard [27]
	Ogun	Edo	Ekiti	Ondo				
SiO_2	53.49	51.60	56.21	49.92	55.98	50.995	60.09	52.90
Al_2O_3	39.90	38.30	28.89	38.98	41.43	42.631	33.23	28.21
Fe_2O_3	0.52	0.54	1.29	0.39	0.608	2.114	2.31	5.31
CaO	0.12	0.22	1.32	1.47	0.056	1.287	0.29	3.0
MgO	0.21	0.16	2.62	0.18	0.496	0.127	0.07	5.21
Na_2O	0.11	0.21	0.05	0.08	0.045	0.284	0.86	-
K_2O	0.53	0.34	0.98	0.93	0.728	0.337	0.43	-
SO_3	0.01	0.06	5.02	2.01	0.313	0.439	-	0.68
Mn_2O	-	-	-	-	0.008	0.006	-	-
ZnO	-	-	-	-	0.002	0.004	0.02	-
P_2O_5	-	-	-	-	0.250	0.051	-	-
TiO_2	-	-	-	-	0.083	1.713	0.16	-
LOI	4.51	2.65	3.57	3.75	-	2.12	2.55	3.9

The findings suggest that the temperature and duration of calcination have a substantial impact on the chemical composition of metakaolin. Beyond 800^{O}C/60mins calcination for all samples, the percentages of the major compounds; Silica and alumina reduced. It was noted that the maximum values of Loss on Ignition (LOI) at 800^{O}C/60mins calcination for all samples are significantly less (4.51, 2.65, 3.57 and 3.75% for Ogun, Edo, Ekiti and Ogun respectively) than the maximum value (6%)

recommended by the codes. Hence, all resulting samples are suitable pozzolans [23]. From Table 6, it could be observed that all samples have similar chemical oxides. However, some trace elements were absent in the study samples.

3.2 Scanning Electron Microscopy of Metakaolin samples analyzed using ImageJ.

The SEM micrographs of all the samples imported to ImageJ are presented in Fig. 2. The SEM images incorporate more fine particles with numerous remaining pores, showing that silica is an active highly porous material with a significant internal surface area. During calcination, the kaolin disintegrates, resulting in a porous structure. The adjusted thresholds of the micrographs are shown in Fig. 3. The histogram, which indicated the frequency of specified ranges of particles present against the area, was plotted using OriginPro software and presented in Fig. 4. This result best explains the particle size distribution of the metakaolin samples.

From Fig. 4a, a total of 765 particles were analyzed for the Ogun sample. The mean area and standard deviation values obtained were 1.481nm² and 18.438 respectively. The percentage of metakaolin particles in the ranges of $0 \geq$ area ≤ 5 nm² was 99.34%, $6.5 \geq$ area ≤ 7 nm² was 0.66%. For the Edo sample, a total of 107 particles were analyzed. The mean area and standard deviation values obtained were 1.703nm² and 4.347 respectively. The percentage of metakaolin particles in the ranges of $0 \geq$ area ≤ 5 nm² was 91.60%, $5 \geq$ area ≤ 10 nm² was 3.74%, $10 \geq$ area ≤ 15 nm² was 2.81%, $15 \geq$ area ≤ 20 nm², and $30 \geq$ area ≤ 35 nm² was 0.96% respectively.

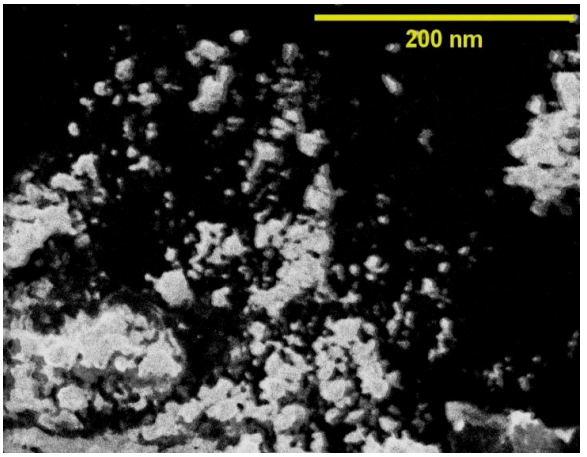

(a)

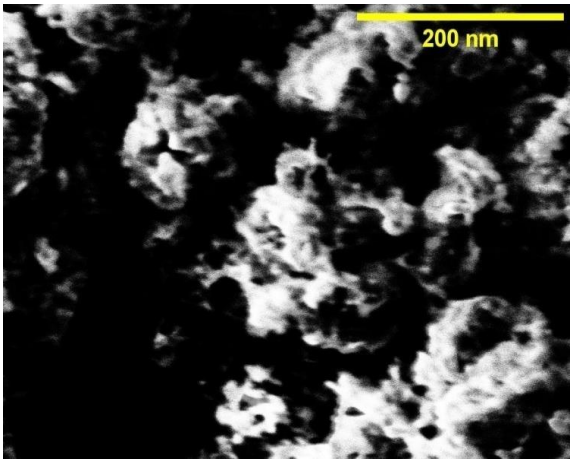

(b)

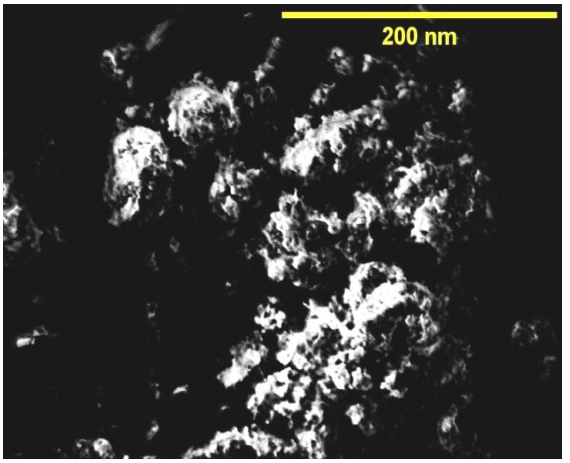

(c)

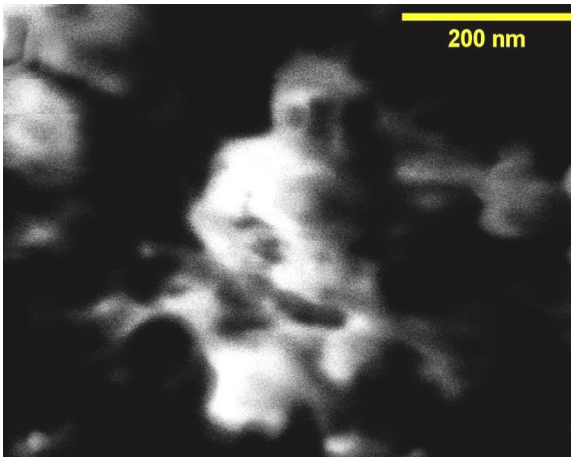

(d)

Fig. 2. SEM images at 100 x magnifications for metakaolin samples (a) Ogun (b) Ekiti (c) Edo (d) Ondo

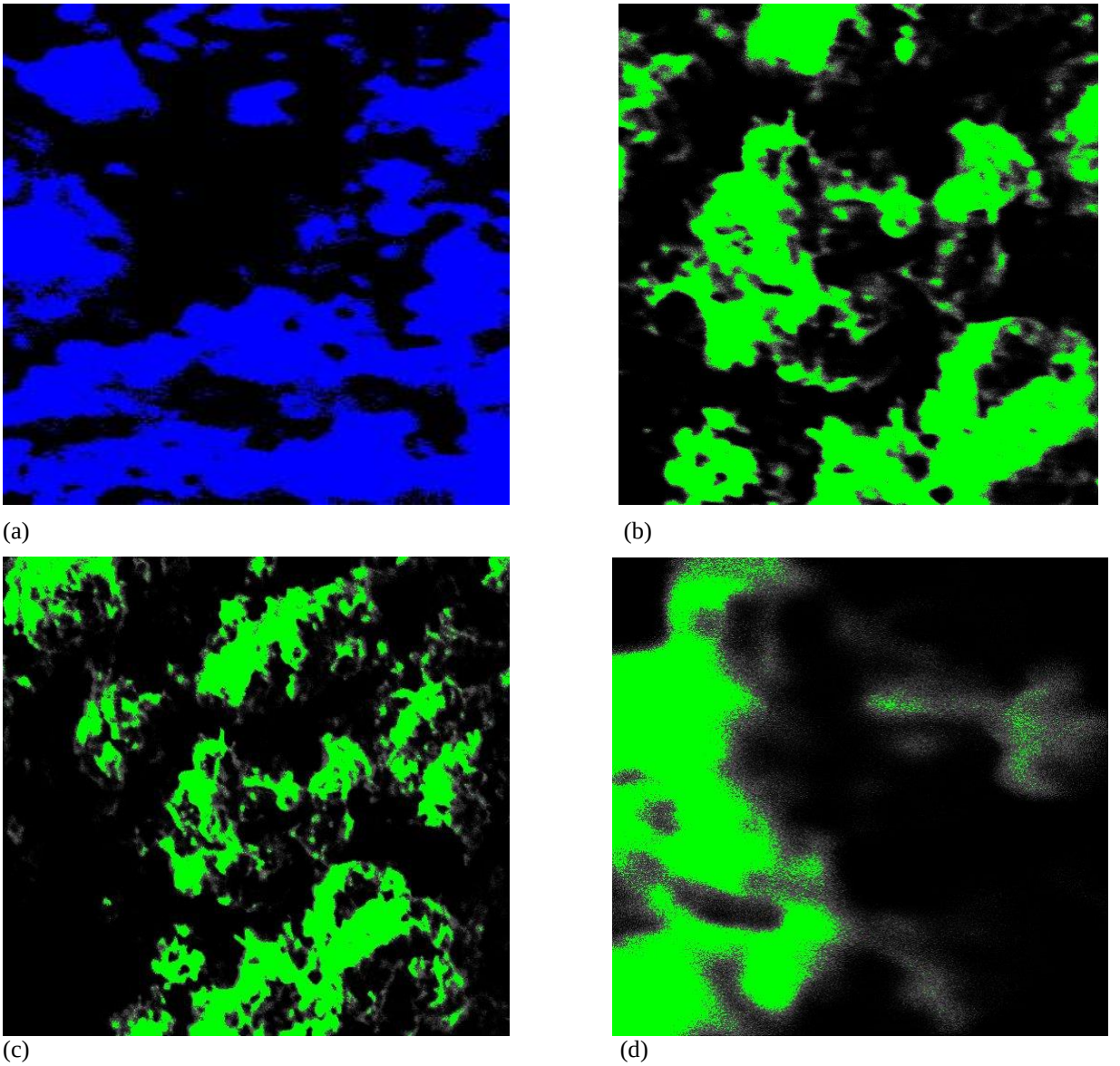

(a) (b)

(c) (d)

Fig. 3. Adjust thresholds of SEM images of Metakaolin samples (a) Ogun (b) Ekiti (c) Edo (d) Ondo

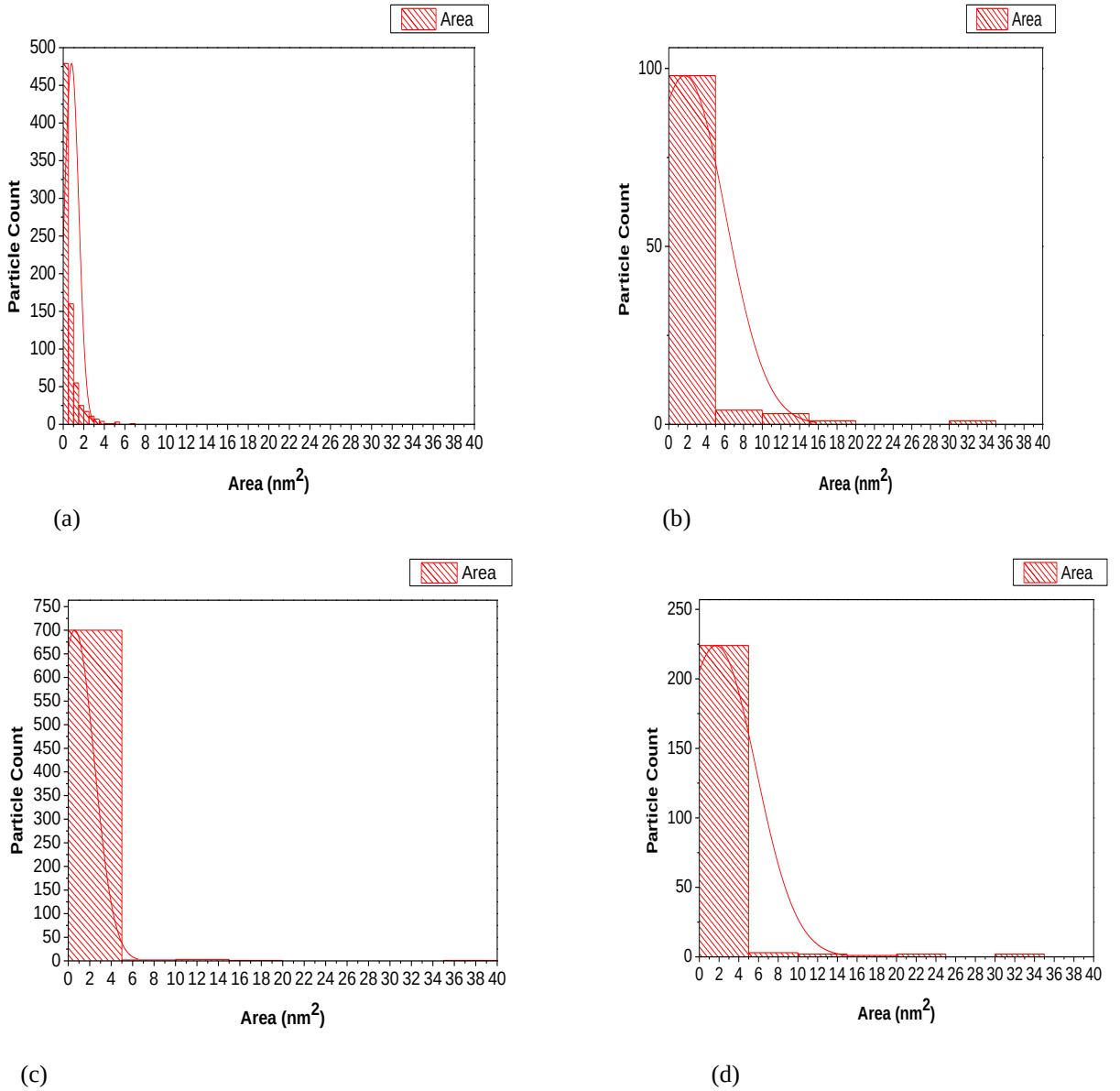

Fig. 4. Particle size distributions of the metakaolin samples (a) Ogun (b) Edo (c) Ekiti (d) Ondo

A total of 713 particles were analyzed for the Ekiti sample. The mean area and standard deviation values obtained were 2.076 nm² and 19.991 respectively. The percentage of metakaolin particles in the ranges of 0 ≥ area ≤ 5 nm² was 98.18%, 5 ≥ area ≤ 10 nm², 15 ≥ area ≤ 20 nm²and 35 ≥ area ≤ 40 nm²were 0.42% respectively while 10 ≥ area ≤ 15 nm² was 0.56%. For the Ondo sample, a total of 239 particles were analyzed. The mean area and standard deviation values obtained were 15.817nm² and 203.909 respectively. The percentage of metakaolin particles in the ranges of 0 ≥ area ≤ 5 nm² was 93.71%, 5 ≥ area ≤ 10 nm² was 2.09%, 10 ≥ area ≤ 15 nm², and 20 ≥ area ≤ 25 nm² were 1.26% respectively, and 15 ≥ area ≤ 20 nm² and 30 ≥ area ≤ 35 nm²were 0.84% respectively.

The results in Fig. 4 showed that the Ogun metakaolin sample has smaller particles compared to other samples and this is an indication that when used in the concrete mix, it would yield better results as the rate of interaction of the metakaolin in the concrete mix would be higher.

3.3 X-Ray Diffraction of Kaolin and Metakaolin samples

XRD test was carried out on raw kaolin samples and the patterns are presented in Fig. 5. Peaks were identified and referenced corresponding to International Centre for Diffraction Data (ICDD) and Crystallography Open Database (COD) card numbers as shown in Table 7. From Table 7, based on the crystal systems identified in the kaolin samples, the crystallographic transformation can be stated as primitive/simple unit cell for Edo, primitive/simple and body-centered cubic unit cell for Ogun and for Ekiti and Ondo kaolin samples, primitive/simple and base centered cubic unit cell were observed respectively [28]. In addition, the Edo (Okpela) sample looked to be heavy due to the presence of just kaolinite. The crystalline phases exhibited by the XRD in the Ogun (Imeko) sample predominantly suggested the presence of kaolinite, quartz, and anatase. Ekiti (Isan-Ekiti) and Ondo (Ifon) share similar properties in that kaolinite predominates, while Illite is also present.

The results differ slightly from those of [29], who used beginning kaolin clay that was mostly kaolinite and quartz. The XRD patterns of the raw kaolin were crystalline as evident by its high-intensity count as seen in the diffractograms displayed. After thermal treatment, an XRD test was performed on calcined clay (metakaolin) to confirm the elimination of kaolinite peaks, and the XRD patterns are shown in Fig. 6. The kaolinite peaks vanished during the calcination process, indicating that kaolinite had completely transformed into metakaolin. Because of the low-intensity count and broad peaks, the XRD diffractograms of metakaolin samples were found to be amorphous. Dehydroxylation causes structural problems in metakaolin by breaking unstable bonds, as seen by the loss of high-order reflections. As a result, as dehydroxylation progressed, the degree of ordering became lower than in kaolinite.

Table 7. Crystalline phases of kaolin

	Edo	**Ogun**	**Ekiti**	**Ondo**
Peaks at 2 θ	12.3856, 21.5375, 25.3174,38.3606, 62.4310	12.3814, 27.0007, 50.2894, 68.5130	12.3765, 25.3043, 38.4592	12.3560, 25.3143, 38.5582
Compound name	Kaolinite	Quartz, Kaolinite, Anatase	Kaolinite, Illite	Kaolinite, Illite
Crystal System/ (Formula)	Anorthic /Triclinic ($Al_2Si_2O_9H_4$)	Hexagonal (Si_3O_6) Anorthic/Triclinic ($Al_2Si_2O_9H_4$) Tetragonal (Ti_4O_8)	Anorthic/ Triclinic($Al_2Si_2O_9H_4$) Monoclinic ($K_2Al_4Si_8O_{24}$)	Anorthic/Triclinic($Al_2Si_2O_9H_4$) Monoclinic ($K_2Al_4Si_8O_{24}$)
Reference code	96-900-9235	96-901-3322 96-900-9235 96-900-8216	96-900-9235 96-901-3733	96-900-9235 96-901-3733
(h,k,l)	0,0,1; 1,1,1; 0,0,2; 1,2,2; 3,3,1	0,0,1; 0,1,2; 0,1,4; 3,3,-1	0,0,1; 0,0,2; 0,1,3	0,0,1; 0,0,2; 0,1,3

After calcination, all of the prominent peaks at 2Θ found in Ogun, Edo, Ekiti, and Ondo kaolin samples vanished. This property is expected due to the OH group collapsing the structure between the plate-like forms of kaolin, resulting in a disordered arrangement. The different modifications could be linked to the crystallographic transition from octahedral to tetrahedral coordination in kaolinite to metakaolin [30]. Scherrer's formula, was used to calculate the crystalline sizes of the metakaolin samples (1).

$$\text{Crystalline Size (Dp)} = \frac{K\lambda}{B\cos\theta} \quad (1)$$

where; K = Scherrer constant (varies 0.68- 2.08),
λ = X-ray wavelength;
Dp = Average crystallite size (nm),
CuKα = 1.54178Å,

B = Full Width at Half Maximum of XRD peak,
θ = XRD peak position; [31].

The crystalline phases of metakaolin samples are shown in Table 8. There were crystal systems transformation observed in metakaolin relative to the kaolin samples.

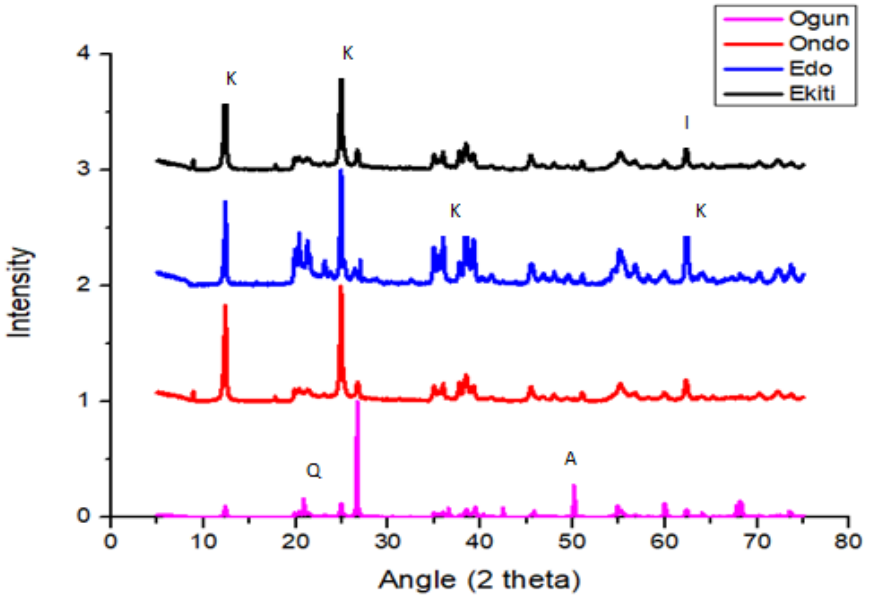

Fig. 5. XRD patterns of kaolin samples (K-Kaolinite; I-Illite; A-Anatase; Q-Quartz)

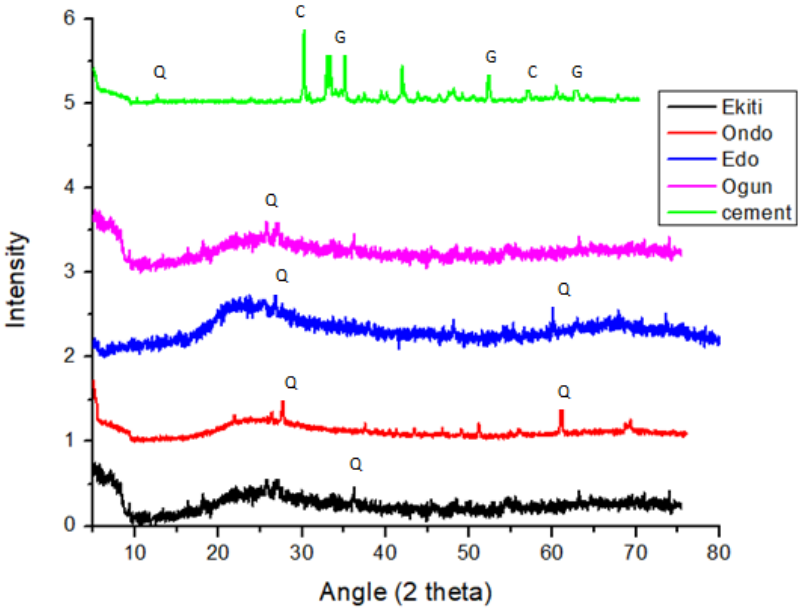

Fig 6. XRD pattern of Metakaolin samples and cement (C-Calcite; G-Gypsum; Q-Quartz)

Table 8. Crystalline phases of Metakaolin at 800^{O}C and 60 minutes heating time

	Edo	Ogun	Ekiti	Ondo
Peaks at 2 θ	25.304, 26.624, 48.037, 50.109	25.272, 26.600, 47.983	25.304, 26.624, 50.109	25.304, 26.624, 48.037, 540.109
Compound name	Anatase Quartz	Anatase Quartz	Anatase Quartz	Anatase Quartz
Crystal System/ (Formula)	Tetragonal (Ti_4O_8) Hexagonal (Si_3O_6)	Tetragonal (Ti_4O_8) Hexagonal (Si_3O_6)	Tetragonal (Ti_4O_8) Hexagonal (Si_3O_6)	Tetragonal (Ti_4O_8) Hexagonal (Si_3O_6)
Reference code	96-900-9087 96-900-9667	96-500-0224 96-901-0145	96-900-9087 96-900-9667	96-900-9087 96-900-9667
(h,k,l)	011, 012, 020, 112	011, 101, 020	011, 012, 112	011, 012, 020, 112

The crystallographic transformation in all the metakaolin samples after the heat treatment at 800^{O}C indicated transformation of studied samples as Edo sample changed from Triclinic to Tetragonal and Hexagonal; Ogun sample from hexagonal/triclinic to tetragonal/hexagonal, Ekiti and Ondo samples triclinic/monoclinic to tetragonal/hexagonal (Tables 7 and 8). This result showed that temperature has a significant effect on the crystallographic transformation of kaolin to metakaolin as confirmed in this study.

3.4 Effect of metakaolin particle size on Mk-GPC compressive strength

Compressive strengths test results obtained in Fig. 7 further justified the particle size distribution analysis carried out using ImageJ and Origin software. The results showed that as the milling duration increased, so did the strength. This is due to the increased surface area of the matrix, which increases the rate of metakaolin interaction in the matrix. This demonstrates that the fineness of metakaolin samples influences the strength of Mk-GPC. The efficiency of dehydroxylation of metakaolin increases with an increase in milling duration. The crucial period for geopolymer concrete was discovered to be within the first week of the mixing-casting process. Geopolymer concrete will perform worse if there isn't a polymeric reaction during this time. Strength development in geopolymer concrete was stable after 28 days, just as it was in standard OPC concrete. The increased polarization of OH during room-temperature curing caused Si-O and Al-O bonds on the Metakaolin surface to break, resulting in higher strength growth [32].

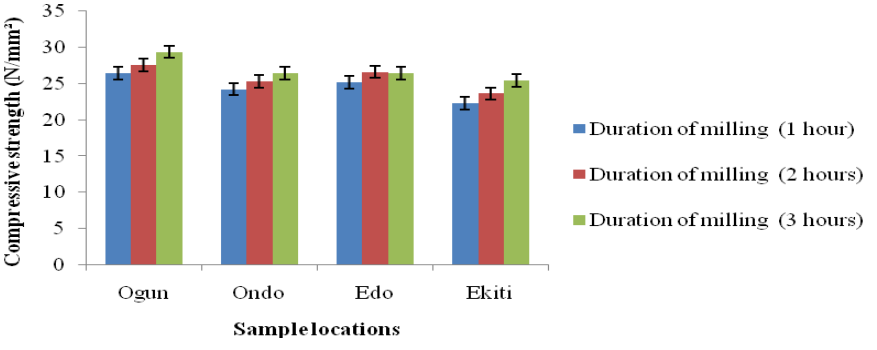

Fig. 7. Effect of metakaolin particle size on Mk-GPC compressive strength.

3.5 Durability studies

The test results as shown in Fig. 8 indicated that Mk-GPC displayed a significant decrease in the flow of charges at 28 days (1155 coulombs; very low) compared to that at 90 days (750 coulombs; low). As the curing days went on, Mk-GPC demonstrated lower Chloride penetrability than control. For the OPC-concrete, a decrease in charge flow was also observed at 28 days (925 coulombs; low) compared to 90 days (835 coulombs; low). These results were rated according to [20] specifications and similar to the results recorded by Rajamane [11] where 722 Coulomb passed through the geopolymer concrete investigated at 90 days and was rated as very low. These showed that both Mk-GPC and OPC-concrete can offer acceptable protection to embedded steel reinforcement from chloride attack in construction works owing to their good resistance to chloride penetration.

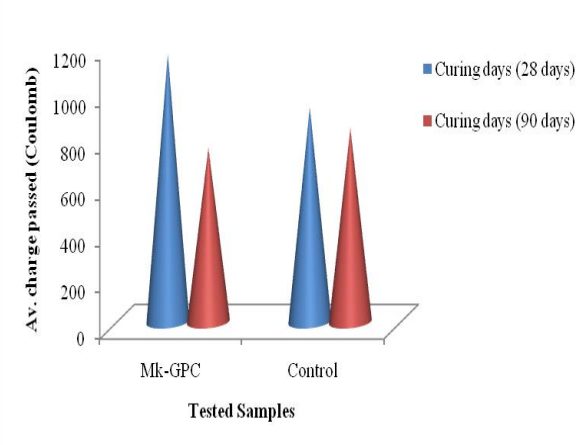

Fig. 8. RCPT of OPC concrete and Mk-GPC

4. Conclusions

The following conclusions can be inferred from the study:

- Varying temperatures on the kaolin samples showed that calcination at 800°C for 60 minutes offered the best results, attributable to the high occurrence of amorphous silica. Also, the total percentages of silica, alumina, and ferric oxide were greater than 70%, the metakaolin samples may be classified as class N pozzolan.
- The crystallographic study of the kaolin and metakaolin samples revealed differences in their characteristics, which might be related to varied environmental and topographical conditions at the kaolin sample source regions.
- Temperature also has significant effect on the crystallographic transformation of kaolin to metakaolin.
- The duration of ball-milling and the particle size of metakaolin have a significant impact on the strength qualities of metakaolin-based geopolymer concrete, according to the findings of this study.
- In the RCPT, Mk-GPC showed lower chloride penetrability than control concrete as the curing days progressed (11.3 percent decrease in chloride penetrability than control at 90-days). Mk-GPC has a better resistance to chloride penetration as a result of this. However, because both Mk-GPC and Ordinary Portland Cement Concrete (control) have strong chloride permeability resistance, they can be deemed suitable for protecting embedded steel reinforcement from corrosion in real-life construction.

Declaration of competing interest

The authors declare that they have no known competing financial interests or personal relationships that could have appeared to influence the work reported in this paper.

References

[1] World Business Council for Sustainable Development, "The Cement Sustainability Initiative. Cement Industry Energy and CO_2 Performance: Getting the Numbers Right,''2009.https://www.wbcsd.org/Sector-Projects/Cement-Sustainability Initiative/Resources/Getting-the-Numbers-Right

[2] Worrell, E., Price, L., Martin, N., Ozawa, M.L., and Hendriks, C., "Carbon Dioxide Emission from the Global Cement Industry,'' *Annual Review of Energy and the Environment*, Vol. 26, No. 1, 2001, pp. 303-329, DOI:10.1146/annurev.energy.26.1.3

[3] Imbabi, M.S., Carrigan, C., and McKenna, S., "Trends and developments in green cement and concrete technology,'' *International Journal of Sustainable Built Environment*, Vol. 1, No. 2, 2012, pp. 194-216, https://doi.org/10.1016/j.ijsbe.2013.05.001

[4] Tafraoui, A., Escadeillas, G., and Vidal, T., "The durability of the Ultra High Performances Concrete containing metakaolin,'' *Construction and building materials*, Vol. 112, 2016, pp. 980-987.

[5] Biljana, R., Alexandra, A., and Ljiljana, R., "Thermal treatment of kaolin clay to obtain Metakaolin," *Institute for Testing of Materials*, Belgrade, Serbia, Vol. 64, No. 4, 2010, pp. 351-356.

[6] Provis, J.L., and Van Deventer, J.S.J., "Geopolymers: structures, processing, properties, and industrial applications," Woodhead Publishing, UK, 2009.

[7] Hardjito, D., and Rangan, B.V., "Development and properties of low calcium fly ash-based geopolymer concrete,'' *Research report GCI*, Curtin University, Perth, 2005.

[8] Barbosa, V.F.F., MacKenzie, K.J., and Thaumaturgo, C., "Synthesis and characterization of materials based on inorganic polymers of alumina and silica: sodium polysialate polymers,'' *Int. J. Inorg. Mater*. Vol. 2, 2009, pp. 309-317.

[9] Vickers, L., Van Riessen, A., and Rickard, W.D., "Fire-resistant geopolymers: role of fibers and fillers to enhance thermal properties," Springer, Singapore, 2015.

[10] Lee, S., Van Riessen, A., Chon, C.M., Kang, N.H., Jou, H.T., and Kim, Y.J., "Impact of activator type on the immobilization of lead in fly ash-based geopolymer,'' *Journal of Hazard Materials*, Vol. 305, 2016, pp. 59-66.

[11] Rajamane, N.P., Nataraja, M.C., Lakshmanan, N., and Dattatreya, J.K., "Rapid chloride permeability test on geopolymer and portland cement concrete,'' *Indian concrete Journal*, 2011, pp. 21- 26.

[12] Wild, S., and Khati, J.M., "Portland consumption in metakaolin cement pastes and mortars,'' *Cem. Concr. Res*. Vol. 27, 1997, pp. 137–146.

[13] Mehta, P.K., Monteiro, P.J.M., "Concrete: Microstructure, Properties, and Materials,'' *Indian Concrete Institute*, First Indian Edition, 2005, pp. 120-122.

[14] Baščarević, Z., "The resistance of alkali-activated cement-based binders to chemical attack, Handbook of Alkali-Activated Cements, Mortars and Concretes,'' Wood head Publishing, pp. 373-396, 2015. ISBN 9781782422761 https://doi.org/10.1533/9781782422884.3.373

[15] Miranda, J.M., Fernandez, J.A., Gonzalez, J.A., and Palomo, A. "Corrosion resistance in Fly ash mortars,'' *Cement and Concrete Research*, Vol. 35, No. 6, 2005, pp. 1210-1217, https://doi.org/10.1016/j.cemconres.2004.07.030

[16] Foraminifera Market Research, *Kaolin Deposits and Mining in Nigeria: The Opportunities*. Retrieved from https://foramfera.com/2016/03/02/kaolin-deposits-and-mining-in-nigeria-the-opportunities/ accessed: 2.03.2017

[17] Gushit, J.S., Olotu, P.N., Maikudi, S., and Gyang, J.D., "Overview of the availability and utilization of kaolin as a potential raw material in chemicals and drug formulation in Nigeria,'' *Continental Journal of Sustainable Development*, Vol. 1, 2010, pp. 17 – 22.

[18] Abiodun, Y.O., Sadiq, O.M., and Adeosun, S.O., "Microstructural, mechanical and pozzolanic characteristics of metakaolin-based geopolymer,'' *Geology, Geophysics and Environment*, Vol. 46, No. 1, 2020, pp. 57-69, https://doi.org/10.7494/geol.2020.46.1.57

[19] Whiting, D., "Rapid Measurement of the Chloride Permeability of Concrete,'' *Public Roads*, Vol. 45, No. 3, 1981, pp. 101-112.

[20] Electrical indication of concrete's ability to resist chloride ion penetration, ASTM International, West Conshohocken, PA, 2012, ASTM C1202, 1994. https://doi.org/10.1520/C1202-94

[21] Poon, C.S., Azhar, S., Anson, M., and Wong, Y.L., "Performance of metakaolin concrete at elevated temperatures,'' *Cement & concrete composites*, Vol. 25, 2003, pp. 83-89.

[22] Standard Specification for coal fly ash and raw or calcined natural pozzolans for use in concrete, ASTM International, West Conshohocken, PA, 2012, ASTM C618, 2012. https://doi.org/10.1520/C0618-12

[23] Shetty, M.S., "Concrete Technology: Theory and Practice.'' Ram Nagar, New-Delhi: S. Chad and Company Ltd, 2009.

[24] Gambo, S., Ibrahim, K., Aliyu, A., Ibrahim, G., and Abdulsalam, H., "Performance of metakaolin-based geopolymer concrete at elevated temperature,'' *Nigerian Journal of Technology*, Vol. 39, No. 3, 2020, pp.732-737.

[25] Albidah, A.S., "Effect of partial replacement of geopolymer binder materials on the fresh and mechanical properties: A review,'' *Ceramics International*, Vol. 47, No. 11, 2021, pp. 14923-14943. https://doi.org/10.1016/j.ceramint.2021.02.127.

[26] Ayeni, O., "Performance of a Nigerian metakaolin, African University of Science and Technology Research,'' *Institutional Repository*, 2017. URI: http://repository.aust.edu.ng/xmlui/handle/123456789/657.

[27] Edouard, J.B., "Experimental evaluation of the durability of fly ash-based geopolymer concrete in the marine environment,'' Florida Atlantic University, ProQuest Dissertations Publishing. 2011.

[28] Online Dictionary of Crystallography (2005), *IUCr*. Accessed on 27March 2022. http://reference.iucr.org/dictionary/Category:Fundamental_crystallography.

[29] Ilic, B.R., Mitrovic, A.A., and Milicic, L.R., "Thermal treatment of kaolin clay.'' *Institute for testing of materials*, Belgrade, Serbia. Vol. 64, No 4, 2010, pp. 351-356.

[30] Cockcroft, J.K., and Barnes, P., "Powder diffraction on the web,'' *Birkbeck College, University of London*, 2016. Accessed on 25 March 2022. http://pd.chem.ucl.ac.uk/pd/welcome.htm

[31] Langford, J.I., and Wilson, A.J.C., "Scherrer after sixty years: A survey and some new results in the determination of crystallite size,'' *Journal of Applied Crystallography*, Vol. 11, 1978, pp. 102-113.

[32] North, M.R., and Swaddle, T.W., "Kinetics of silicate exchange in alkaline aluminosilicate solutions,'' *Inorganic Chemistry*, Vol. 39, 2000, pp. 2661-2665.